Journal of Microbiological Methods 157 (2019) 123–130

Contents lists available at ScienceDirect

Journal of Microbiological Methods

journal homepage: www.elsevier.com/locate/jmicmeth

Assessment of white rot fungus mediated hardwood degradation by FTIR spectroscopy and multivariate analysis

Darshan M. Rudakiya, Akshaya Gupte*

Department of Microbiology, N. V. Patel College of Pure and Applied Sciences, Vallabh Vidyanagar, Anand 388 120, Gujarat, India

ARTICLE INFO

Keywords:
FTIR spectroscopy
Hardwood
Multivariate analysis
White rot fungi

ABSTRACT

Evaluating the biomass degradation using fast, validate and sensitive techniques for exploratory purposes of biofuel production has been developed since last decade. Thus, we assessed the degradation of two Indian hardwoods using FTIR and chemometric approaches. Two white rot fungi, namely *Pseudolagarobasidium acaciicola* AGST3 and *Tricholoma giganteum* AGDR1, were selected among twenty-one fungal isolates for higher hardwood degradation. In the screening, *P. acaciicola* AGST3 and *T. giganteum* AGDR1 depicted the dry woody mass loss of 20.51% and 22.38%, respectively. Cellulose crystallinity of *P. acaciicola* AGST3 treated hardwoods was 4-fold lower than untreated hardwoods, showing the higher cellulose degradation efficiency. *P. acaciicola* AGST3 treated samples exhibited maximum deviation of guaiacyl units of lignin, cellulose and hemicelluloses. *T. giganteum* AGDR1 treated hardwoods showed maximum deviation of guaiacyl- and syringyl- units of lignin and hemicelluloses. Multivariate approach revealed the degradation patterns and preferences are varied based on the fungi and hardwood. The approach used in the present study can certainly distinguish the variations among the different biomass samples that having similar composition. Additionally, higher lignin degradability of these fungi can be used in biomass pretreatment, which significantly utilized to produce second-generation biofuels.

1. Introduction

Woody biomass is the most abundant feedstock and organic source on the Earth, producing about 5.64×10^{10} tons of carbon and 1.08×10^{11} tons of oil equivalents (Taha et al., 2016; Couturier et al., 2018). This biomass has been envisioned for the development of modern bio-based refineries, which produce the second-generation biofuels i.e. hydro-treating oil, bio-oil, Fischer–Tropsch oil, bio-ethanol, bio-butanol, mixed oils (Tiwari et al., 2018). The advantages of second-generation biofuels are: a) biomass is not competing with food; b) newly developed technologies which reduce the cost of fuel, and c) it is environmental friendly for the fuel generation (Naik et al., 2010). Several pre-treatments have been used to transform into biofuels, biogas and other value-added products, wherein fungal pretreatment is a “green” approach with lower energy input and chemical addition (Masran et al., 2016; Rouches et al., 2016). Wood decay fungi considerably alter the mechanical properties of wood, wherein the wood type, wood structure, decay type and fungal species are the core benchmarks to evaluate the extent of wood damage (Gilani et al., 2017). Several studies have concentrated on the use of wood decay fungi for the degradation of wood components (Pandey and Pitman, 2003; Lehringer et al., 2011; Skyba et al., 2016). Due to the wood degradation using white rot fungi, enhance the properties of thermal reaction, specifically pyrolysis reaction, which makes reaction faster for bio-oil production and other value added products (Rudakiya and Gupte, 2017). Value added products mainly contains carboxylic acids, lignin monomers, benzofurans, benzaldehydes, ferulic acid, etc. (Masran et al., 2016; Tiwari et al., 2018).

Conventionally, wood decay has been divided into major three types: white rot, brown rot and soft rot. This classification is based on the ability to degrade lignin with cellulose and/or hemicelluloses (Schwarze, 2007). Among them, white rot decay is mainly caused by majority of basidiomycetes as they mineralize the lignin moieties and turn the wood into white biomass (Rudakiya and Gupte, 2017). White rot fungi have whole “wood decaying machinery” i.e. lignocellulolytic enzymes, reactive oxygen species, organic acids, organohalogen metabolites, etc., which make the white rot fungi dexterous to mineralize the wood components (Manavalan et al., 2015; Xu et al., 2015; Gahlout et al., 2017). White rot fungi are subdivided into two major groups based on their ability to attack on lignin selectively or simultaneously with carbohydrates. In simultaneous rot, degradation of lignin, cellulose and hemicelluloses occurs simultaneously, while lignin degrades earlier than cellulose and hemicelluloses in selective delignification (Schwarze, 2007; Gilani et al., 2017).

* Corresponding author at: Head, Department of Microbiology, N. V. Patel College of Pure & Applied Sciences, Vallabh Vidyanagar, 388 120 Anand, Gujarat, India.
E-mail address: akshaya_gupte@hotmail.com (A. Gupte).

https://doi.org/10.1016/j.mimet.2019.01.007
Received 26 July 2018; Received in revised form 11 January 2019; Accepted 14 January 2019
Available online 16 January 2019

Fourier transform Infrared (FTIR) spectroscopy is a fast, simple, non-destructive and useful analytical technique, which is successfully applied to characterize the wood structural chemistry for several decades (Pandey and Pitman, 2003; Lazzari et al., 2018). Moreover, this technique offers the qualitative and quantitative analysis with the minimum use of wood sample (Traoré et al., 2016). Conventionally, FTIR is frequently used for the identification and abundance of functional groups of wood components, relative changes of lignin/carbohydrate and variations in control and decayed wood samples (Pandey and Pitman, 2003). However, minor changes in FTIR spectra of different samples cannot be identified visually, so multivariate statistics is applied to unravel the divergence among the samples (Chen et al., 2010). More recently, few studies used the integrated approach of FTIR and PCA analysis to reveal the FTIR fingerprints among different samples (Plácido and Capareda, 2014; Lazzari et al., 2018). Hardwoods used in the present study, *Pithecellobium dulce* and *Tamarindus indica* possess the similar composition of wood components, consequently this holistic approach can be useful to understand the variation among untreated and fungal treated wood samples (Rudakiya and Gupte, 2017). Initially, we have screened the potential white rot fungi, which can competently degrade the hardwoods. Furthermore, this study is mainly concentrated to identify and to characterize the degradation of two Indian hardwoods using FTIR and multivariate analysis.

2. Materials and methods

2.1. Chemicals, media and hardwoods

Sabouraud dextrose broth, malt extract, agar-agar and other chemicals used for the screening and degradation study were purchased from Hi-media, India. Eight to ten years old *Pithecellobium dulce* and *Tamarindus indica* were used, wherein the sapwood of hardwoods was cut and ground into small particles. Furthermore, these particles were sieved to a uniform particle size of 4–5 mm. Mixture of both hardwood particles were used for primary and secondary screening study.

2.2. White rot fungal cultures

Some white rot fungal cultures were previously isolated in our laboratory, which are: *Pleurotus ostreatus* AGHP (GeneBank: EU420068), *Tricholoma giganteum* AGHP (GeneBank: KT154749), *Pseudolagarobasidium acaciicola* AGST3 (GeneBank: HQ323693) and *Schizophylum commune* AGMJ1 (GeneBank: JQ023130). The remaining cultures (*Trametes serialis*, *T. hersuta*, *P. ostreatus*, *T. versicolor* and *Phanerochaete chrysosporium*) were procured from the culture collection centers. List of pure cultures of fungi used in the present study are shown in Table 1. All fungal cultures were maintained by sub-culturing on malt extract agar containing streptomycin (25 µg/ml) at 30 °C for 15 days.

2.3. Isolation and screening of white rot fungi

Fruiting bodies of mushroom samples were collected from the nearby vicinity of Changa, Anand and Vallabh Vidyanagar (Gujarat, India) **(Fig. S1)**. Fresh tissues of the fruiting bodies were sterilized using mercuric chloride (1 g/l) for 4–5 min followed by washing with distilled water. Sterilized samples were incubated on Sabouraud dextrose agar plates containing 25 µg/ml of streptomycin for 15 days and transferred repeatedly until pure culture obtained. All fungal cultures were initially screened by growing the cultures on the moistened hardwood particles (wood to moisture ratio = 1:4 (*w/v*)) in 250 ml Erlenmeyer flasks for 30 days. After incubation, all myco-wood samples were harvested, and fungal biomass was estimated using the method described by Rodríguez-Couto et al. (2009).

After primary screening, white rot fungi were grown again on the mixed hardwood particles for 30 days and estimated the dry mass loss,

Table 1
Response of isolated fungal cultures during primary and secondary screening for hardwood degradation after 30 days of incubation.

Isolate code/fungal name	Primary screening	Secondary screening
	Fungal growth on hardwood (g %)[a]	Dry mass loss (%)[a]
Unidentified cultures		
AGDR1	6.85 ± 0.21**	22.38 ± 0.40***
AGDR2	3.52 ± 0.09	5.60 ± 0.14
AGDR3	4.95 ± 0.14*	14.75 ± 0.29*
AGDR4	5.10 ± 0.11*	11.12 ± 0.42*
AGDR5	1.49 ± 0.04	2.34 ± 0.20
AGDR6	0.38 ± 0.009	1.13 ± 0.11
AGDR7	4.62 ± 0.32*	4.36 ± 0.38
AGDR8	3.99 ± 0.16	10.84 ± 0.64*
AGDR9	0.41 ± 0.09	2.40 ± 0.17
AGDR10	0.97 ± 0.03	1.24 ± 0.10
AGDR11	5.98 ± 0.17**	10.01 ± 0.18*
AGDR12	0.84 ± 0.1	0.78 ± 0.06
Identified cultures		
Pleurotus ostreatus AGHP	5.99 ± 0.21**	12.11 ± 0.87*
Trametes serialis	3.13 ± 0.09	5.59 ± 0.43
Trametes hersuta	5.87 ± 0.11**	6.31 ± 0.26
Tricholoma giganteum AGHP	5.13 ± 0.14*	10.38 ± 0.98*
Pseudolagarobasidium acaciicola AGST3	7.32 ± 0.22***	20.51 ± 1.09**
Pleurotus ostreatus	6.17 ± 0.15**	8.36 ± 0.76
Trametes versicolor	5.34 ± 0.08*	14.22 ± 0.96*
Phanerochaete chrysosporium	6.33 ± 0.26**	12.60 ± 0.34*
Schizophylum commune AGMJ1	6.87 ± 0.12**	1.58 ± 0.06

*P < .1, **P < .01, ***P < .001.

[a] Mixture of both hardwood particles (*P. dulce* and *T. indica*) were used for the primary and secondary screening.

wherein wood samples were cleaned by brushing followed by washing with distilled water. Control and degraded wood particles were oven-dried at 80 °C for 4–5 h to remove excessive moisture. Afterwards, samples were prepared according to TAPPI T 257 cm-02 (TAPPI, 2002). The mass loss (%) of respective hardwoods was analyzed using the method described by Rudakiya and Gupte (2017). One-way ANOVA with Newman-Keuls's multiple comparisons test of wood degradation was performed, wherein significance level of alpha was 0.05. Furthermore, the molecular identification of unidentified fungal isolate (AGDR1) was achieved by extracting the fungal genomic DNA and amplifying ITS4 and ITS5 region. After obtaining sequences from NCBI database, phylogenetic trees were constructed and analyzed using MEGA v7.0.

2.4. Degradation of hardwoods by white rot fungi

In 250 ml Erlenmeyer flask, 5 g of oven dried hardwood particles (*T. indica* and *P. dulce*) were autoclaved for 60 min at 121 °C and 15 psi. Similarly, Asther's medium was autoclaved in 250 ml Erlenmeyer flask for 15 min and supplemented 20 ml of medium in the flasks containing hardwood particles to maintain the substrate to moisture ratio of 1:4 (*w/v*) (Asther et al., 1988). Furthermore, five plugs of *Pseudolagarobasidium acaciicola* AGST3 and *Tricholoma giganteum* AGDR1 inoculated on the moistened wood particles and incubated at 28 °C for 30 days.

2.5. FTIR spectroscopy analysis

After 30 days of incubation, fungal treated and untreated wood samples were washed twice with deionized water and dried at 80 °C for 4–5 h to remove the excessive moisture. The dried sample was pulverized into fine powder (40 mesh screen) and mixed with KBr crystals and compressed into pellets at 1.5 MPa pressure. The spectra were acquired in triplicates, with 16 scans and spectral resolution of 2 cm^{-1}, which

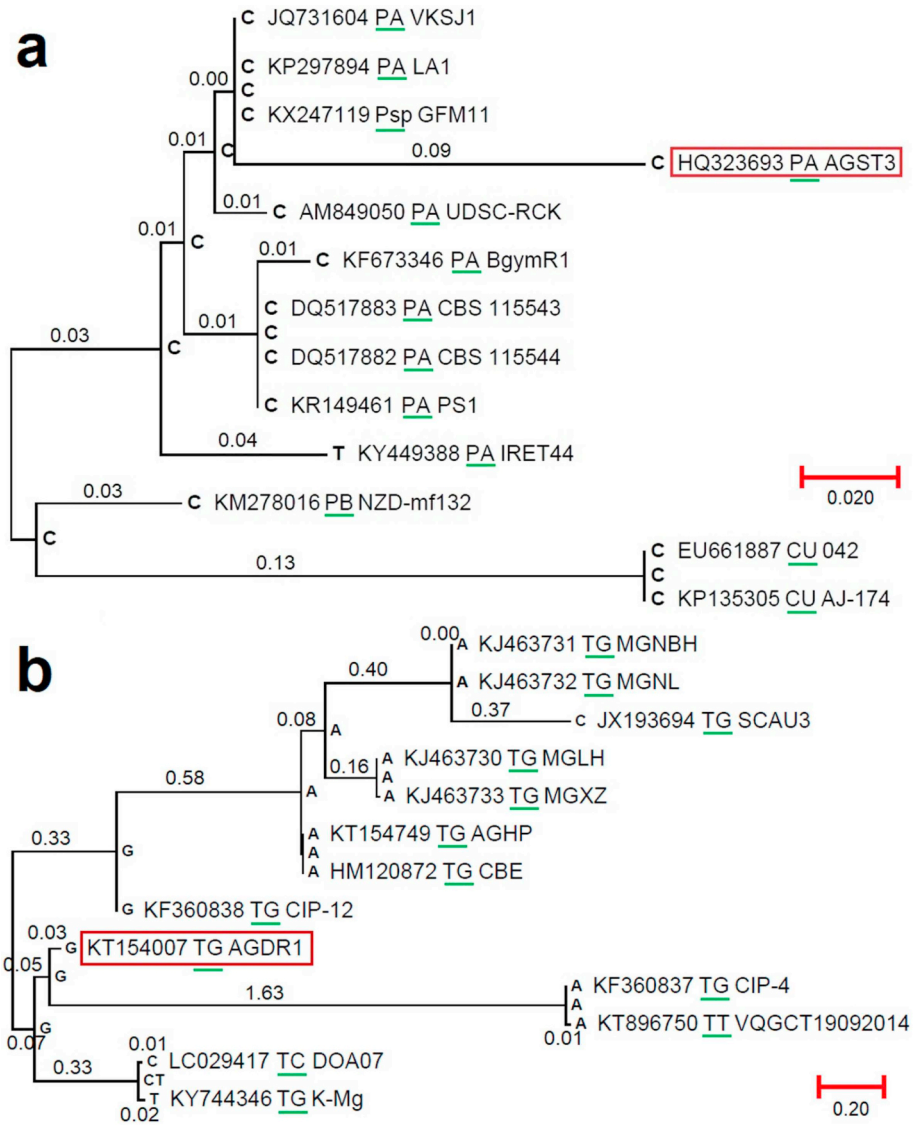

Fig. 1. Evolutionary history and ancestral state of both white rot fungi, *P. acaciicola* AGST3 and *T. giganteum* AGDR1, were inferred using the Maximum Likelihood method based on the Tamura-Nei mode, wherein 500 replicates were used to construct bootstrapped consensus tree. Evolutionary and ancestral analysis was conducted in MEGA v7.0. Initial code represents in each branch is GeneBank accession numbers of representative organism, which is followed by the green underlined codes depict the Genus and species name of organism. PA: *Pseudolagarobasidium acaciicola*; Psp: *Pseudolagarobasidium* sp.; PB: *Pseudolagarobasidium belizense*; CU: *Cerrena unicolor*; TG: *Tricholoma giganteum*; TT: *Tricholoma titans* and TC: *Tricholoma crassa.* (For interpretation of the references to colour in this figure legend, the reader is referred to the web version of this article.)

measured in the range of 400–4000 cm^{-1} using Spectrum GX spectrophotometer (Perkin Elmer, USA). Reference absorbance peaks of the cellulose, hemicelluloses and lignin was used to evaluate the cellulose crystallinity and lignin to carbohydrate ratio, which is described by Shi and Li (2012) and Zeng et al. (2012). Subsequently, the absorbance data of respective FTIR samples was transformed into matrices to construct the principal component analysis (PCA) plots (Rudakiya, 2018). One-way ANOVA with Dunnett's multiple comparisons test was performed using GraphPad Prism v7.0, wherein the data were considered significant when $p \leq .05$. Hierarchical Cluster Analysis (HCA) of untreated and fungal treated wood samples was carried out based on the group average cluster method in Origin v9.5 and Euclidean distance matrix was used to plot the dendrogram.

3. Results and discussion

3.1. Screening of white rot fungi

For several decades, two-step screening method has been used to screen the efficient lignin degrading fungi. The fungal growth rate is evaluated initially, in which faster and efficient growth means appropriate penetration of fungal mycelia in wood tissue. The rate of wood degradation was calculated thereafter (Li et al., 2008). Fungi form the mycelial networks efficiently in the wood tissue to degrade the lignin, cellulose and hemicelluloses by secreting the enzymes, free radicals, organic acids, etc. (Rudakiya and Gupte, 2017). Total of twenty-one fungal isolates (twelve unidentified and nine identified fungal cultures) were used for the screening purpose. Among them, thirteen fungi were able to colonize the hyphae efficiently on hardwood particles, showing the higher growth on the selected hardwoods. In secondary screening, five unidentified and five identified fungal cultures exhibited the > 10% of dry mass loss (Table 1). Two cultures, *Pseudolagarobasidium acaciicola* AGST3 and AGDR1 isolate depicted the maximum dry mass loss of 20.51 ± 1.09% and 22.38 ± 0.40%, respectively (**Fig. S2**). By using similar methodology, Li et al. (2008) have screened the novel fungus, *Fusarium concolor* with efficient selective lignin degradation capability.

3.2. Identification and characterization of selected fungi

P. acaciicola AGST3, a novel white rot fungus, belongs from newly classified Cerrenaceae family. It exhibits 97% identity with 93% of query coverage with *P. acaciicola* VKSJ1 (GeneBank: JQ731604) (Justo et al., 2017). Evolutionary and ancestral analysis of both white rot fungi is shown in Fig. 1. Evolutionary and ancestral state analysis was suggested that the ancestral similarity of *P. acaciicola* AGST3 was higher with other *P. acaciicola* strains. However, the evolutionary distance of *P. acaciicola* AGST3 is higher as compared to other strains. Molecular

Table 2
Classification, morphological and microscopic characters of selected wood decaying fungi.

Parameters	*Pseudolagarobasidium acaciicola* AGST3	*Tricholoma giganteum* AGDR1
Fruiting body		
Fungal growth on Sabouraud dextrose agar	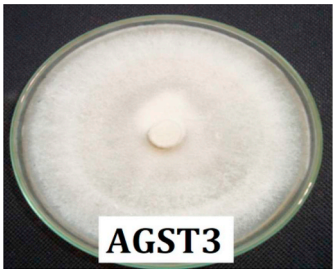	
Scanning electron micrograph[a]	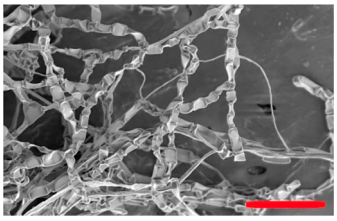	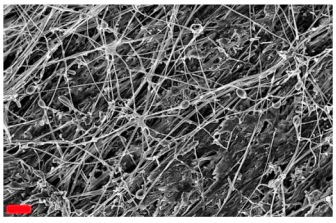
Classification		
Kingdom	Fungi	Fungi
Phylum	Basidiomycota	Basidiomycota
Class	Agaricomycetes	Agaricomycetes
Order	Polyporales	Agaricales
Family	Cerrenaceae	Catathelasmataceae
Genus	*Pseudolagarobasidium*	*Tricholoma*
Species	*acaciicola*	*giganteum*
Strain	AGST3	AGDR1

[a] Scale bar in scanning electron micrograph of *P. acaciicola* AGST3 = 10 μm and *T. giganteum* AGDR1 = 20 μm.

identification of AGDR1 isolate was further corroborated by sequencing its ITS4 and ITS5 genes at Agharkar Research Institute (Pune, India). Further, the isolate was identified as a *Tricholoma giganteum* AGDR1 (GeneBank: KT154007), exhibiting 99% identity with 98% of query coverage with *T. giganteum* CBE Coimbatore (GeneBank: HM120872). Evolutionary distance of *T. giganteum* AGDR1 is higher and deviated with other *T. giganteum* strains. Similarly, ancestry of *T. giganteum* AGDR1 is disparate from other related *T. giganteum* strains (AGHP and CBE Coimbatore). Unusual ancestry and deviated evolutionary distance revealed the uniqueness of the strain among *T. giganteum* strains.

Morphological and microscopic characteristics revealed that both fungi had distinct morphology of fruiting body, on agar plates and microscopic features. The fruiting body of AGDR1 isolate revealed that cap is convex, and gills are not attached with the stem. *T. giganteum* AGDR1 has 15–22 cm long basidiocarps, as the complete development of basidiocarps is observed in most Agaricales (Alexopoulos, 1962). Different stages of the fruiting body of *T. giganteum* AGDR1 are shown in Table 2. The microscopic examination of *T. giganteum* AGDR1 showed the clamp connections forming generative aseptate hypha and was found to be sporulating. On the contrary, *P. acaciicola* AGST3 has a mushroom like fruiting body with 4–6 cm of basidiocarp (Justo et al., 2017). The fruiting body of *P. acaciicola* AGST3 revealed that cap is depressed and adnexed gills are observed. Additionally, this fungus showed septate hyphae with clamp connections and different size of spores under scanning electron micrograph.

3.3. Composition of hardwoods

In case of untreated *P. dulce* and *T. indica,* both the hardwoods contained 30% of total lignin, wherein acid insoluble lignin (Klason lignin) and acid soluble lignin were 24–25% and 4–5%, respectively. In addition, hemicelluloses, cellulose, extractives and ash of the both hardwoods were 21–22%, 41–43%, 2–3% and 1–2%, respectively (**Fig. S3)**. The composition of untreated *P. dulce* and *T. indica* was nearly similar. It might be possible as they were belonging from the same family. In case of *P. dulce* degradation, *P. acaciicola* AGST3 exhibited the degradation of lignin, cellulose and hemicellulose were 37% and 10% 18% respectively. However, *T. giganteum* AGDR1 showed up to 49%, 17% and 12% of lignin, cellulose and hemicelluloses, respectively. Similar results were obtained by various researchers, wherein simultaneous rot exhibited the higher lignin degradation as compared to the cellulose degradation (Manavalan et al., 2015; Karim et al., 2016; Masran et al., 2016).

3.4. FTIR spectroscopy analysis

The FTIR spectroscopy determines the intensities of cellulose, hemicellulose and lignin bands, which show the possible degradation or modification of wood components (Traoré et al., 2016). The aromatic structure intensities and functional group identification of untreated and fungal treated wood samples were studied using FTIR technique. FTIR spectrum of the untreated and fungal treated wood samples is

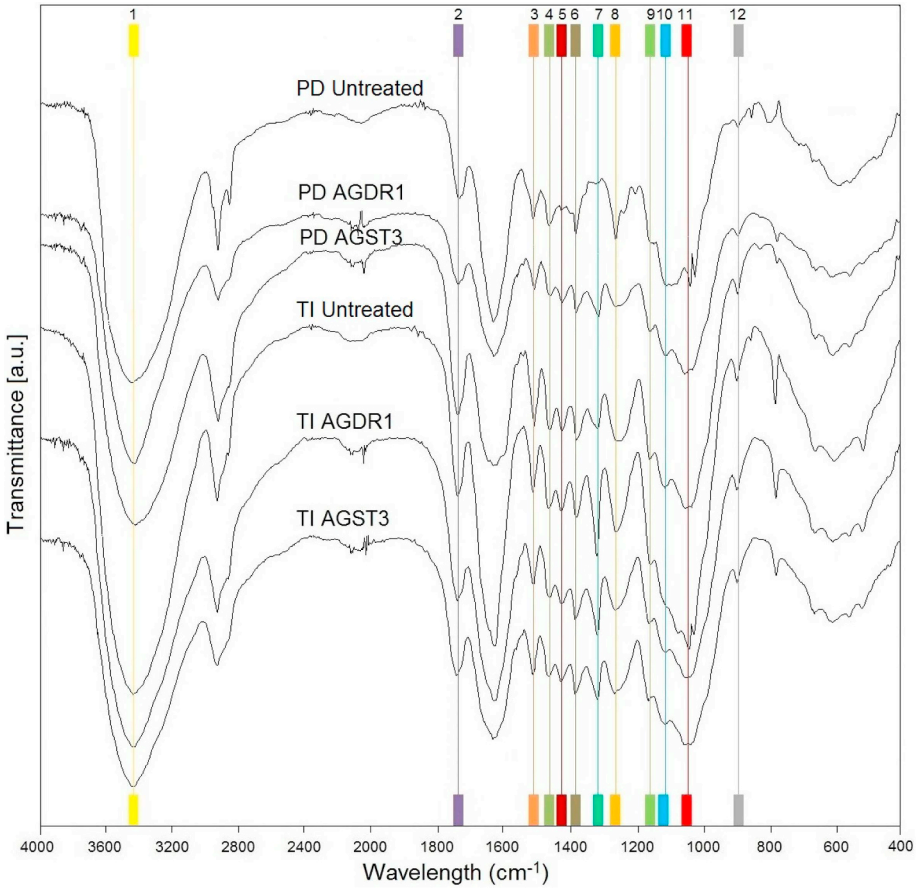

Fig. 2. FTIR spectra of untreated and fungal treated *P. dulce* and *T. indica*. Twelve different peaks are highlighted in different colors and wavelength assignment of the following peak numbers showed in Table 3. (PD/TI AGDR1 = wood samples pretreated by *T. giganteum* AGDR1 for 30 days, PD/TI AGST3 = wood samples pretreated by *P. acaciicola* AGST3 for 30 days).

Table 3
FTIR spectrum wavelength assignment and their shift difference of untreated and fungal treated *P. dulce* and *T. indica*.

Peak no.	Wavelength Assignment	*P. dulce*			*T. indica*		
		Untreated	AGST3[b]	AGDR1[b]	Untreated	AGST3	AGDR1
1	O_2-H_2…O_6 intramolecular stretching modes in cellulose	3435.93	−11.81	−11.32[a]	3429.83	+11.12	+2.13[a]
2	Unconjugated C=O in xylans (hemicellulose)	1734.80	+3.43	+3.53	1736.42	+5.31	+1.66
3	Aromatic skeletal ring in lignin	1511.19	−2.45	−3.01	1510.18	−0.98	−0.51
4	C-H deformation of lignin and carbohydrates	1464.88	−0.95	−3.11	1463.96	−2.73	−3.65
5	C-H deformation of lignin and carbohydrates	1427.84	−3.76	−2.91	1425.30	+0.38	−2.24
6	C-H deformation in cellulose and hemicellulose	1384.20	−1.55	−0.52	1380.66	+2.91	+2.79
7	C_1-O vibrations in syringyl units and C-H vibrations in cellulose	1321.28	−2.95	−5.11	1318.25	−1.38	−1.24
8	C-O stretch in lignin and C-O linkage in guaiacyl aromatic groups	1263.60	−3.08	+0.91	1260.72	+4.52	+2.42
9	C-O-C vibrations in cellulose and hemicellulose	1158.10	+2.98	+3.35	1158.10	+4.09	+4.09
10	Aromatic skeletal and C-O stretch in lignin	1112.63	+1.08	−1.52	1112.21	−1.10	+0.94
11	C-O stretch in cellulose and hemicellulose	1039.23	−3.73	−7.82	1040.38	−4.18	–
12	C-H deformation in cellulose	896.55	+1.15	+0.81	897.43	−1.62	−0.62

[a] Shift difference (shift increase +, shift decrease –) in the respective wavelength peak of fungal treated wood compared to untreated wood.
[b] AGDR1 and AGST3 referred as the respective woods were pretreated by *P. acaciicola* AGST3 and *T. giganteum* AGDR1.

shown in Fig. 2. The wavelength assignments of lignin, cellulose and hemicelluloses associated bands and their shift differences are summarized in Table 3. In *P. dulce,* the aromatic skeletal vibrations of lignin were shifted higher in *T. giganteum* AGDR1 (−3.01) than *P. acaciicola* AGST3 (−2.45). In contrast, the aromatic skeletal vibrations of lignin shifted higher in *P. acaciicola* AGST3 (−0.98) treated than *T. giganteum* AGDR1 (−0.45) treated *T. indica* wood. Likewise, deviation of cellulose assignments (C−H deformation and stretching vibrations) was higher in *P. acaciicola* AGST3 than *T. giganteum* AGDR1 treated hardwood samples. In case of hemicelluloses assignments, *T. giganteum* AGDR1 and *P. acaciicola* AGST3 exhibited higher deviation in *P. dulce* and *T. indica* hardwood, respectively. Similarly, Karim et al. (2016) revealed that *Pleurotus ostreatus* degraded the lignin and cellulose of oak wood at the same rate analyzed by FTIR spectroscopy.

Relative changes in the intensity of the lignin/carbohydrates (cellulose and hemicelluloses) of untreated and fungal treated wood samples are shown in Fig. 3. To carry out relative intensity of lignin/carbohydrates, a prominent and specific peak of lignin is mandatory; hence, most of the peaks in the fingerprint region of FTIR spectra contribute for all the wood components. So, 1510 cm^{-1} has been selected as it has no significant contribution for the cellulose and hemicelluloses (Zeng et al., 2012). Similarly, the peak description of the wavelength which corresponded for carbohydrates (1737, 1383, 1162 and 897 cm^{-1}) is given in Table 3.

Results of relative intensity revealed that the progressively intensity of lignin was decreased in fungal treated samples than untreated

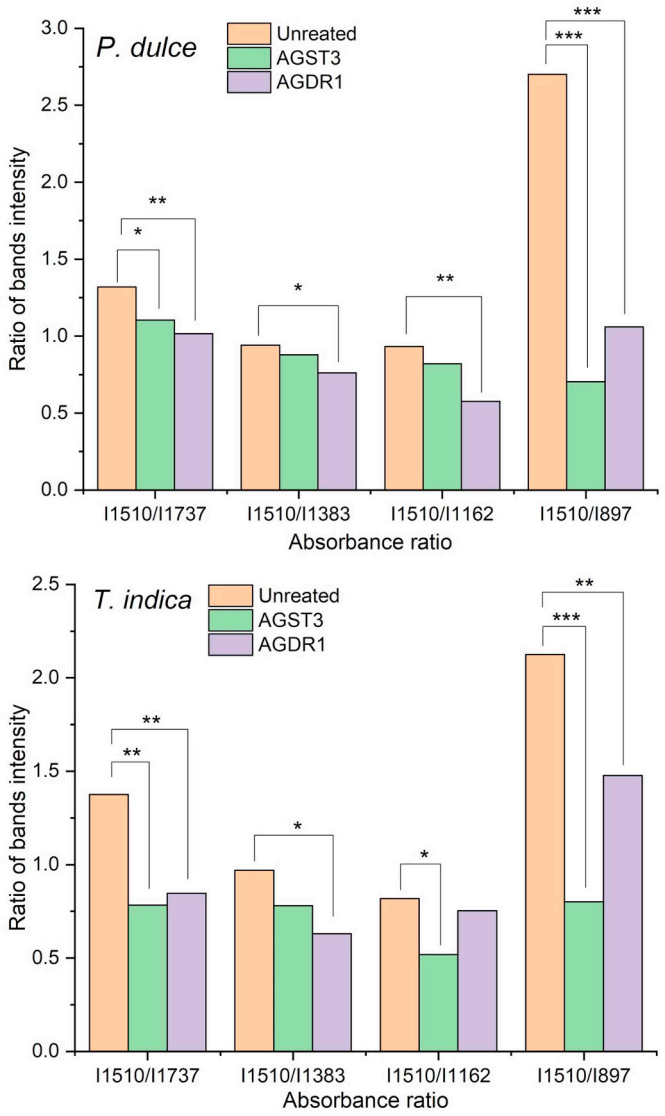

Fig. 3. Relative intensity of the lignin associated with cellulose and hemicelluloses (carbohydrates) for untreated and fungal treated (AGDR1 and AGST3) hardwoods. AGDR1 and AGST3 referred as the respective woods were pretreated by *P. acaciicola* AGST3 and *T. giganteum* AGDR1. $*P < .1$, $**P < .01$, $***P < .001$ compared with untreated hardwoods.

samples, showing the both fungi acted on the lignin moieties of hardwoods. Preceding results suggested that both fungi depicted the simultaneous degradation of cellulose and hemicelluloses with lignin, which was evident from the ratio obtained from 1737 cm^{-1} and other carbohydrate peaks (Zeng et al., 2012). These researchers also obtained the similar results of degradation ratio, depicting that *E. taxodii* 2538 and *I. lacteus* CD2 had the selective and simultaneous degradation capability of bamboo, respectively. *T. giganteum* AGDR1 has low capability for the degradation of *P. dulce* and *T. indica* cellulose as compared to *P. acaciicola* AGST3. These results agree with our previous study, wherein compositional study of hardwood suggested that *P. acaciicola* has higher cellulose degrading capability due to the secretion of high amounts of cellulases (Rudakiya and Gupte, 2017). *P. acaciicola* AGST3 showed the high I_{1510}/I_{1737} ratio in *P. dulce* as compared to *T. indica*, depicting the higher hemicelluloses degradation observed in *T. indica* compared to *P. dulce*.

To assess the crystallinity of cellulose, the ratio of 1427 cm^{-1} and 896 cm^{-1} was used for the untreated and fungal treated hardwood samples. The I_{1427}/I_{896} ratio revealed that *P. acaciicola* AGST3 (0.612) and *T. giganteum* AGDR1 (0.854) treated *P. dulce* samples exhibited lower ratio compared to untreated samples (1.217). A similar trend was observed in case of *T. indica*, wherein *P. acaciicola* AGST3 (1.036) showed lower cellulose crystallinity than *T. giganteum* AGDR1 (1.246). Similarly, *Phanerochaete chrysosporium* and *Gloeophyllum trabeum* treated bamboo samples showed the lower cellulose crystallinity than control bamboo samples (Xu et al., 2013). These findings indicated that both fungi were able to degrade the cellulose with lignin and hemicelluloses; however, *P. acaciicola* AGST3 was efficiently degraded cellulose than *T. giganteum* AGDR1.

Briefly, FTIR findings suggested the decay preference and pattern of wood components by fungi. *P. acaciicola* AGST3 and *T. giganteum* AGDR1 exhibited the simultaneous degradation of lignin, cellulose and hemicellulose, although the degradation capabilities of wood components differed according to the type, structure and species of fungi and hardwood (Traoré et al., 2016; Gilani et al., 2017). *T. giganteum* AGDR1 showed higher degradation of lignin and hemicelluloses compared to cellulose in *P. dulce* samples, however higher lignin degradation is observed compared to cellulose and hemicelluloses in *T. indica* wood samples. Likewise, *P. acaciicola* AGST3 exhibited higher degradability of cellulose than lignin and hemicelluloses in *P. dulce* wood, while higher lignin and cellulose degradation is exhibited compared to hemicelluloses in *T. indica*.

3.5. Principal component analysis (PCA)

PCA is the one of the largely used multivariate statistic method, which directly applied in industry to improve process control, economics and product diversity (Chen et al., 2010; Krasznai et al., 2018). Variance of PC1 and PC2 for *P. dulce* and *T. indica* were 94.6% & 1.7% and 93.1% & 2.7%, respectively. Scores of PC1 and PC2 and their corresponding wavelength assignments are given in Fig. 4. In case of *P. dulce*, C—O and aromatic stretching of lignin components, C—H deformation of lignin, cellulose and hemicelluloses and C-O-C vibrations of cellulose and hemicelluloses were highly deviated in case of *T. giganteum* AGDR1 treated samples, suggesting the higher degradation of lignin and hemicelluloses components compared to *P. acaciicola* AGST3 treated samples. Surprisingly, C—H deformation vibrations of cellulose of *T. giganteum* treated samples were less deviated than *P. acaciicola* treated samples, showing the higher efficacy of cellulose degradation by *P. acaciicola* AGST3. In case of *P. acaciicola* AGST3, stretching vibrations of lignin components were less deviated to untreated *P. dulce* lignin vibrations, revealing the lignin degradation were less compared to *T. giganteum* AGDR1.

Untreated and fungal treated *T. indica* samples were depicted the diverged trend than *P. dulce* samples. Lignin component vibrations of *T. giganteum* AGDR1 were less deviated from the untreated samples, revealing the lesser degradation of lignin observed by *T. giganteum* AGDR1. C—O, O-H-O and C═O stretching vibrations of cellulose and hemicelluloses and stretching vibrations of syringyl and guaiacyl units were highly deviated from untreated samples, suggesting the *P. acaciicola* AGST3 exhibited higher degradation of lignin, cellulose and hemicelluloses. Stretching vibrations of hemicellulose of *T. giganteum* AGDR1 treated samples were highly deviated than cellulose and lignin stretching and deformation vibrations. Higher degradation of hemicelluloses is obtained as compared to cellulose and lignin of *T. indica* by *T. giganteum* AGDR1. Plácido and Capareda (2014) identified the variations of CGT biomass components at different pretreatments using PCA analysis. Similarly, pyrolytic bio-oil composition of different biomasses has been used for PCA analysis to classify the biomass (Lazzari et al., 2018).

3.6. Hierarchical cluster analysis (HCA)

The HCA emphasizes the natural grouping of the data in large data set, presenting as a dendrogram to visualize the clusters and distance

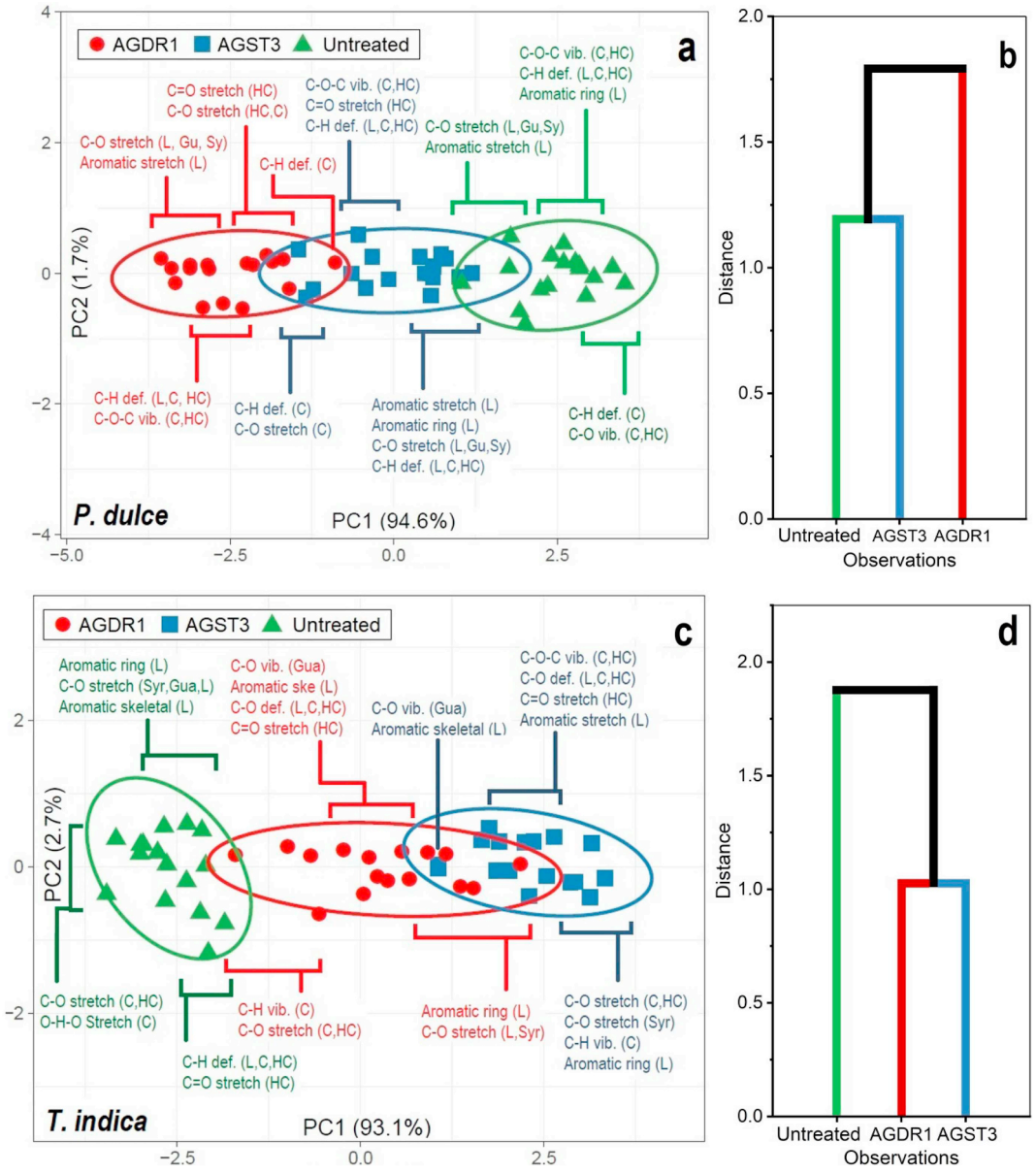

Fig. 4. Principal component analysis (PCA) (a, c) and Hierarchical Cluster Analysis (HCA) (b, d) of untreated and fungal treated *P. dulce* (a, b) and *T. indica* (c, d), depicting the divergence among untreated, AGST3 and AGDR1 treated samples. Variance of each principal component is displayed in the respective axis and prediction eclipses of respective groups with 95% of probability. AGDR1 and AGST3 referred as the respective woods were pretreated by *P. acaciicola* AGST3 and *T. giganteum* AGDR1. L, lignin; HC, hemicelluloses; C, cellulose; Syr, Syringyl and Gua, guaiacyl.

among different groups (Chen et al., 2010). In the present work, we used group average cluster's method with Euclidean distance as the similarity measurement. The dendrogram of HCA analysis clearly depicted the main two clusters in both hardwoods (Fig. 4). HCA analysis of *P. dulce* revealed that untreated and *P. acaciicola* AGST3 treated samples showed 1.191 of distance and *T. giganteum* AGDR1 exhibited 1.793 of distance, respectively. Results suggested that *T. giganteum* AGDR1 treated *P. dulce* samples were more diverge as compared to *P. acaciicola* AGST3 treated woods, depicting that *T. giganteum* AGDR1 was most efficiently acted on the *P. dulce*. On the contrary, *P. acaciicola* AGST3 and *T. giganteum* AGDR1 treated *T. indica* wood presented the similar distance of 1.014 compared to untreated *T. indica* (1.888). These results suggested that both fungi acted similarly on *T. indica* wood samples; however, the degradation capability of wood components was different. Similar methodology was applied by Chen et al. (2010), wherein HCA of FTIR data for different wood samples and detergent fibers were clustered into two main groups, depicting the divergence among the sample composition. Similarly, heterogeneity of oat and pea roots was carried out using cluster analysis of FTIR spectra, depicting the clear discrimination of two major group oat and pea roots (Naumann et al., 2010). These results indicate that HCA is an independent method, which provides the similarities and distance among the various samples.

4. Conclusions

In the present study, potential white rot fungi were isolated from the different localities and screened for the efficient hardwood degradation. After quantitative and qualitative screening, *P. acaciicola* AGST3 and *T. giganteum* AGDR1 were found to be efficient hardwood degraders among fungal isolates. FTIR and multivariate analysis suggested that both fungi could degrade the lignin, cellulose and hemicelluloses simultaneously, though the degradation efficacy was different. *P. acaciicola* AGST3 and *T. giganteum* AGDR1 acted efficiently on the lignin of

P. dulce and *T. indica*, respectively. *P. acaciicola* AGST3 efficiently degraded the cellulose of both Indian hardwoods. The cultures used in the present study have shown their higher efficacy towards lignin degradation, which can further use for the pre-treatment of second-generation biofuels.

Acknowledgement

The authors are very obliged to Charutar Vidhya Mandal and Sophisticated Instrumentation Centre for Applied Research & Testing (SICART), V.V. Nagar for providing the necessary instrumentation facilities.

Conflict of interest

On behalf of all authors, the corresponding author states that there is no conflict of interest.

Appendix A. Supplementary data

Supplementary data to this article can be found online at https://doi.org/10.1016/j.mimet.2019.01.007.

References

Alexopoulos, C.J., 1962. Introductory Mycology. John Wiley & Sons, New York.
Asther, M., Lesage, L., Drapron, R., Corrieu, G., Odier, E., 1988. Phospholipid and fatty acid enrichment of *Phanerochaete chrysosporium* INA-12 in relation to ligninase production. Appl. Microbiol. Biot. 27, 393–398.
Chen, H., Ferrari, C., Angiuli, M., Yao, J., Raspi, C., Bramanti, E., 2010. Qualitative and quantitative analysis of wood samples by Fourier transform infrared spectroscopy and multivariate analysis. Carbohyd. Polym. 82, 772–778.
Couturier, M., Ladevèze, S., Sulzenbacher, G., Ciano, L., et al., 2018. Lytic xylan oxidases from wood-decay fungi unlock biomass degradation. Nat. Chem. Biol. 14, 306–310.
Gahlout, M., Rudakiya, D.M., Gupte, S., Gupte, A., 2017. Laccase-conjugated amino-functionalized nanosilica for efficient degradation of Reactive Violet 1 dye. Int. Nano Lett. 7, 195–208.
Gilani, M.S., Heeb, M., Huch, A., Fink, S., Schwarze, F.W.M.R., 2017. Fracture in Norway spruce wood treated with *Physisporinus vitreus*. Wood Sci. Technol. 51, 195–206.
Justo, A., Miettinen, O., Floudas, D., Ortiz-Santana, B., Sjökvist, E., Lindner, D., et al., 2017. A revised family-level classification of the Polyporales (Basidiomycota). Fungal Biol. 121, 798–824.
Karim, M., Daryaei, M.G., Torkaman, J., Oladi, R., Ghanbary, M.A.T., Bari, E., 2016. In vivo investigation of chemical alteration in oak wood decayed by *Pleurotus ostreatus*. Int. Biodeter. Biodegr. 108, 127–132.
Krasznai, D.J., Hartley, R.C., Roy, H.M., Champagne, P., Cunningham, M.F., 2018. Compositional analysis of lignocellulosic biomass: conventional methodologies and future outlook. Crit. Rev. Biotechnol. 38, 199–217.
Lazzari, E., Schena, T., Marcelo, M.C.A., Primaz, C.T., Silva, A.N., Ferrão, M.F., Bjerk, T., Caramão, E.B., 2018. Classification of biomass through their pyrolytic bio-oil composition using FTIR and PCA analysis. Ind. Crop. Prod. 111, 856–864.
Lehringer, C., Saake, B., Živković, V., Richter, K., Militz, H., 2011. Effect of *Physisporinus vitreus* on wood properties of Norway spruce. Part 2: aspects of microtensile strength and chemical changes. Holzforschung 65 (5), 721–727.
Li, L., Li, X.Z., Tang, W.Z., Zhao, J., Qu, Y.B., 2008. Screening of a fungus capable of powerful and selective delignification on wheat straw. Lett. Appl. Microbiol. 47, 415–420.
Manavalan, T., Manavalan, A., Heese, K., 2015. Characterization of lignocellulolytic enzymes from white-rot fungi. Curr. Microbiol. 70, 485–498.
Masran, R., Zanirun, Z., Bahrin, E.K., Ibrahim, M.F., Yee, P.L., Abd-Aziz, S., 2016. Harnessing the potential of ligninolytic enzymes for lignocellulosic biomass pretreatment. Appl. Microbiol. Biot. 100, 5231–5246.
Naik, S.N., Goud, V.V., Rout, P.K., Dalai, A.K., 2010. Production of first and second generation biofuels: a comprehensive review. Renew. Sust. Energ. Rev. 14, 578–597.
Naumann, A., Heine, G., Rauber, R., 2010. Efficient discrimination of oat and pea roots by cluster analysis of Fourier transform infrared (FTIR) spectra. Field Crop Res. 119, 78–84.
Pandey, K.K., Pitman, A.J., 2003. FTIR studies of the changes in wood chemistry following decay by brown-rot and white-rot fungi. Int. Biodeter. Biodegr. 52, 151–160.
Plácido, J., Capareda, S., 2014. Analysis of alkali ultrasonication pretreatment in bioethanol production from cotton gin trash using FT-IR spectroscopy and principal component analysis. Bioresour. Bioprocess. 1, 23. https://doi.org/10.1186/s40643-014-0023-7.
Rodríguez-Couto, S., Osma, J.F., Toca-Herrera, J.L., 2009. Removal of synthetic dyes by an eco-friendly strategy. Eng. Life Sci. 9, 116–123.
Rouches, E., Herpoël-Gimbert, I., Steyer, J.P., Carrere, H., 2016. Improvement of anaerobic degradation by white-rot fungi pretreatment of lignocellulosic biomass: a review. Renew. Sust. Energ. Rev. 59, 179–198.
Rudakiya, D.M., 2018. Metal tolerance assisted antibiotic susceptibility profiling in *Comamonas acidovorans*. Biometals 31, 1–5.
Rudakiya, D.M., Gupte, A., 2017. Degradation of hardwoods by treatment of white rot fungi and its pyrolysis kinetics studies. Int. Biodeter. Biodegr. 120, 21–35.
Schwarze, F.W.M.R., 2007. Wood decay under the microscope. Fungal Biol. Rev. 21, 133–170.
Shi, J., Li, J., 2012. Metabolites and chemical group changes in the wood-forming tissue of *Pinus koraiensis* under inclined conditions. Bioresources 7, 3463–3475.
Skyba, O., Cullen, D., Douglas, C.J., Mansfield, S.D., 2016. Gene expression patterns of wood decay fungi *Postia placenta* and *Phanerochaete chrysosporium* are influenced by wood substrate composition during degradation. Appl. Environ. Microb. 82, 4387–4400.
Taha, M., Foda, M., Shahsavari, E., Aburto-Medina, A., Adetutu, E., Ball, A., 2016. Commercial feasibility of lignocellulose biodegradation: possibilities and challenges. Curr. Opin. Biotech. 38, 190–197.
TAPPI standard, 2002. T 257 Cm-02, Sampling and Preparing for Wood Analysis.
Tiwari, R., Nain, L., Labrou, N.E., Shukla, P., 2018. Bioprospecting of functional cellulases from metagenome for second generation biofuel production: a review. Crit. Rev. Microbiol. 44, 244–257.
Traoré, M., Kaal, J., Cortizas, A.M., 2016. Application of FTIR spectroscopy to the characterization of archeological wood. Spectrochim. Acta A 153, 63–70.
Xu, G., Wang, L., Liu, J., Wu, J., 2013. FTIR and XPS analysis of the changes in bamboo chemical structure decayed by white-rot and brown-rot fungi. Appl. Surf. Sci. 280, 799–805.
Xu, P., Leng, Y., Zeng, G., Huang, D., et al., 2015. Cadmium induced oxalic acid secretion and its role in metal uptake and detoxification mechanisms in *Phanerochaete chrysosporium*. Appl. Microbiol. Biot. 99, 435–443.
Zeng, Y., Yang, X., Yu, H., Zhang, X., Ma, F., 2012. The delignification effects of white-rot fungal pretreatment on thermal characteristics of moso bamboo. Bioresour. Technol. 114, 437–442.